Article

Synthesis and Properties of Shape Memory Poly(γ-Benzyl-L-Glutamate)-*b*-Poly(Propylene Glycol)-*b*-Poly(γ-Benzyl-L-Glutamate)

Lin Gu [1,2,†], Yuanzhang Jiang [1,†] and Jinlian Hu [1,*] (iD)

[1] Institute of Textiles & Clothing, The Hong Kong Polytechnic University, Hong Kong 999077, China; lin.gu@polyu.edu.hk (L.G.); yuan-zhang.jiang@connect.polyu.hk (Y.J.)
[2] Key Laboratory of Marine Materials and Related Technologies, Key Laboratory of Marine Materials and Protective Technologies of Zhejiang Province, Ningbo Institute of Materials Technology and Engineering, Chinese Academy of Sciences, Ningbo 315201, China
[*] Correspondence: jin-lian.hu@polyu.edu.hk; Tel.: +852-2766-6437
[†] These authors contributed equally to this work.

Abstract: Shape memory polymers (SMPs) have attracted much attention as an important class of stimuli-responsive materials for biomedical applications. For SMP-based biomaterials, in addition to suitable shape recovery performances, their mechanical properties, biodegradability, biocompatibility, and sterilizability needs to be considered. Polypeptides can satisfy the requirements outlined above. However, there are few reports on shape memory polypeptides. In this paper, shape memory poly(γ-benzyl-L-glutamate) (PBLG-PPG-PBLG) was synthesized by ring-opening polymerization of γ-benzyl-L-glutamate-*N*-carboxyanhydrides (BLG-NCA) with poly(propylene glycol) bis(2-aminopropyl ether) as the macroinitiator. [1]H Nuclear Magnetic Resonance (NMR) and Fourier-Transform Infrared Spectroscopy (FTIR) were used to characterize the structure of the obtained PBLG-PPG-PBLG. The FTIR analysis showed that PBLG-PPG-PBLG has α-helical and β-sheet structures. PBLG-PPG-PBLG has good shape memory properties, its shape recovery time is less than 120 s, and its shape recovery rate is 100%. In this study, we reported a simple synthetic method to obtain intelligent polypeptide materials, which will be used in many biomedical applications.

Keywords: ring-opening polymerization; shape memory; poly(γ-benzyl-L-glutamate); biomedical application

1. Introduction

In recent years, shape memory polymers (SMPs) have attracted much attention owing to their excellent properties and potential applications such as biomedical devices, actuators, textiles, and packaging materials [1–3]. SMPs have an ability to change their shapes from temporary to original upon external stimuli, such as heat, light, and pH [4–7]. Among them, thermo-triggered SMPs are the most widely studied, and a number of thermally-actuated SMPs have been reported, such as polyurethanes, polyesters, polyacrylates, polynorbornene, and polyimide [8–14]. Typical thermo-responsive SMPs could be described as a netpoint-switch model as reported in our previous work [15], where the netpoints could be of physically or chemically cross-linking, determining permanent shapes, and the switches refer to amorphous or crystallization soft phase responsible for temporary shapes. Inspired by spider silks, we recently reported shape memory biopolymers based on β-sheet structures of polyalanine segments [16]. The β-sheet structures act as netpoints responsible for the achievement of excellent shape recovery ability and high shape fixity.

Polypeptide is one of the most important synthetic protein-mimicking materials that consist of a specific amino acid sequence linked by peptide bonds, which has been widely used in various applications such as gene delivery, drug delivery, and tissue engineering [17,18]. The sequences could adopt secondary structures of *α*-helices, *β*-sheets, etc., through hydrogen bonds within peptide backbones, enabling interesting self-assembly behaviors and bioactivity of polypeptides [19,20]. Currently, ring-opening polymerization (ROP) of *N*-carboxyanhydrides (NCAs) has been the most common method used for large scale preparation of high molecular weight polypeptides [18]. Many stimuli-responsive polypeptides have been prepared by the ROP of *α*-amino acid NCAs based on the conformational transitions between secondary structures [21–24]. However, there are few reports on shape memory polypeptide. For SMPs-based biomaterials, in addition to suitable shape recovery performances, their mechanical properties, biodegradability, biocompatibility, and sterilizability need to be considered [25]. Polypeptides can satisfy the outlined above requirements. In this work, shape memory poly(*γ*-benzyl-L-glutamate) (PBLG-PPG-PBLG) was synthesized, and its second structure and properties were studied. This work will provide new insight for designing shape memory biopolymers, and promote the development of interdisciplinary subjects of bionics and intelligent materials.

2. Experimental Section

2.1. Materials

γ-Benzyl-L-glutamate (BLG) and triphosgene were purchased from J & K Scientific Ltd. (Beijing, China). and recrystallized prior to use. Poly(propylene glycol) bis(2-aminopropyl ether) (PPG-diamine 400, average M_n ~400) was obtained from Aldrich and dried at 100 °C in vacuum for 4 h before use. Tetrahydrofuran (THF), *N,N*-dimethylformamide (DMF), and hexane were dried over CaH_2 and distilled prior to use. Other reagents were used as received.

2.2. Preparation of PBLG-PPG-PBLG and Film

γ-Benzyl-L-glutamate-*N*-carboxyanhydride (BLG-NCA) was synthesized from BLG and triphosgene in dried THF according to the literature [26]. BLG-NCA was recrystallized from THF/hexane (*v/v*, 1/3) and dried at 50 °C in vacuum, as confirmed by [1]H Nuclear Magnetic Resonance (NMR) spectroscopy (see Figure 1).
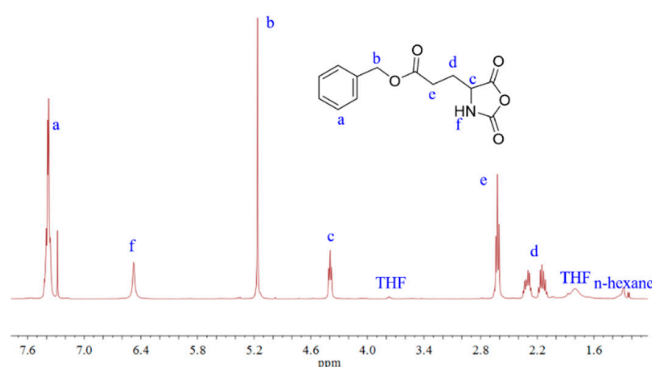

Figure 1. [1]H Nuclear Magnetic Resonance (NMR) spectrum of *γ*-Benzyl-L-glutamate-*N*-carboxyanhydride (BLG-NCA) in $CDCl_3$. THF: Tetrahydrofuran.

PBLG-PPG-PBLG was synthesized by ring-opening polymerization of BLG-NCA using PPG-diamine 400 as the initiator in dried DMF. In a nitrogen gas Schlenk line, 10 g BLG-NCA, 0.783 mL PPG-diamine 400, and 100 mL DMF were introduced into a 0.5-L flask free of water and oxygen. The reaction was carried out at room temperature for 72 h. After that, the reaction mixture was precipitated using diethyl ether, filtered and dried to constant weight in vacuum.

The obtained PBLG-PPG-PBLG was dissolved in chloroform to form a 10 wt % solution. The solution was then poured into a Teflon mold and dried at room temperature for 24 h, and then further dried in vacuum at 60 °C for 24 h. Finally, the PBLG-PPG-PBLG film with a thickness of ~0.4 mm was prepared.

2.3. Characterization

^{1}H NMR spectra were obtained in deuterated chloroform (CDCl$_3$) or trifluoroacetic acid (CF$_3$COOD) using Avance III 400 MHz spectrometer (Bruker, Billerica, MA, USA). Fourier transform infrared (FTIR) spectra were collected on a Spectrum 100 FTIR spectrometer (PerkinElmer, Waltham, MA, USA). Differential scanning calorimetry (DSC) analysis was performed on a DSC 8000 instrument (PerkinElmer, Waltham, MA, USA) at a rate of 20 °C min^{-1} under a N$_2$ atmosphere from -30 °C to 200 °C. Thermogravimetric analysis (TGA) was carried out on a thermal analyzer (METTLER TOLEDO, Columbus, OH, USA) at a heating rate of 10 °C min^{-1} under a N$_2$ atmosphere from 50 °C to 600 °C. Tensile test was conducted on an Instron 5566 instrument (Instron, Norwood, MA, USA) with a speed of 10 mm/min at 25 °C.

The bending test was empolyed to quantitatively evaluate the shape memory behavior of the PBLG-PPG-PBLG film. Firstly, the straight specimen was heated at 100 °C for 5 min, and then bent to an angle (θ_0) close to 180 °. Subsequently, it was cooled down to room temperature with an external force to maintain the deformation (θ_i). Then the deformed specimen was heated to 100 °C, and recording the change of the angle (θ_f) with time. The shape fixity ratio (R_f) and shape recovery ratio (R_r) could be calculated according to the following formulas:

$$R_f = \frac{\theta_i}{\theta_0} \times 100\%$$

$$R_r = \frac{\theta_i - \theta_f}{\theta_i} \times 100\%$$

3. Results and Discussion

As shown in Scheme 1, shape memory PBLG-PPG-PBLG was synthesized by the ring-opening polymerization of BLG-NCA using PPG (Poly Propylene Glycol)-diamine 400 as an initiator. ^{1}H NMR and FTIR spectra were used to characterize the structure of the obtained PBLG-PPG-PBLG. Figure 2 shows the ^{1}H NMR spectrum of PBLG-PPG-PBLG in CF$_3$COOD. The characteristic resonances at 7.0 ppm and 4.9 ppm are assigned to CH$_2$ and phenyl in benzyl group, respectively, and that at 4.4 ppm is assigned to CH groups in amide linkage, while the signals at 3.2–3.8 ppm are assigned to CH and CH$_2$ groups in the PPG units. The molecular weight of the obtained PBLG-PPG-PBLG was calculated to be ~5000 according to the integral area, which is close to the theoretical value.
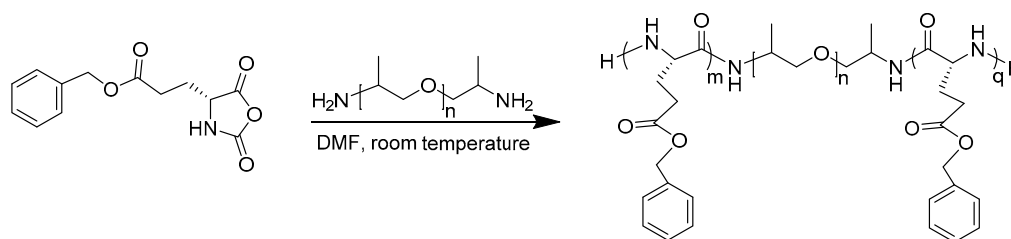
Scheme 1. Synthesis of shape memory poly(γ-benzyl-L-glutamate) (PBLG-PPG-PBLG). DMF: *N,N*-dimethylformamide.
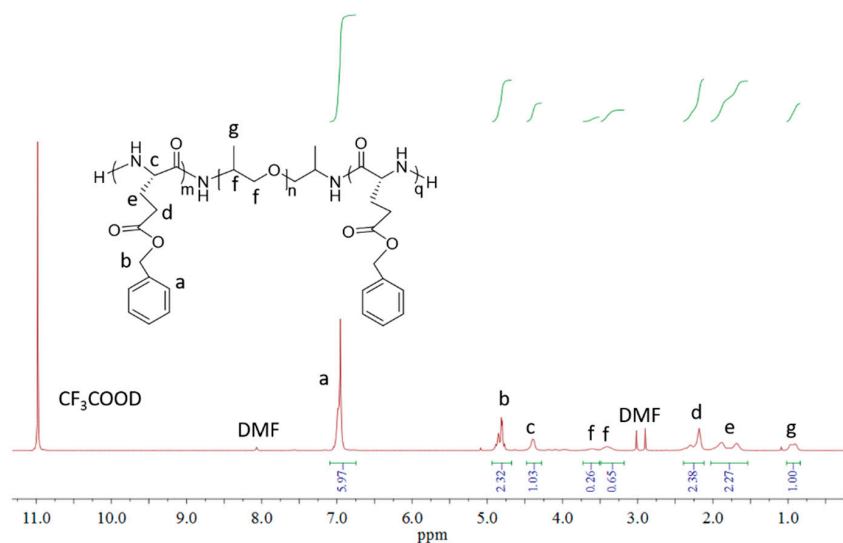
Figure 2. ^{1}H NMR spectrum of PBLG-PPG-PBLG in trifluoroacetic acid (CF$_3$COOD).

Figure 3 exhibits the FTIR spectrum of the resulting PBLG-PPG-PBLG. The amide I (backbone C=O stretch) region is present at 1600–1700 cm^{-1}, which could be used to determine the structure (e.g., α-helix, β-sheet) of polypeptides [27]. The strong band of α-helix occurs at ~1668 cm^{-1} (left-handed) or ~1655 cm^{-1} (right-handed). The amide I peak is located at lower wavenumbers for a parallel β-sheet (1636–1640 cm^{-1}) compared to an antiparallel β-sheet (1622–1632 cm^{-1}) [27]. It can be clearly observed from Figure 3 that the obtained PBLG-PPG-PBLG not only forms right-handed α-helix, but also has antiparallel β-sheet structure, as reported for PBLG-*b*-poly(dimethylsiloxane)-*b*-PBLG [28]. The percent of β-sheet conformation was calculated to be ~5.12% by the deconvolution of the amide I region (1620–1670 cm^{-1}). Moreover, the strong absorptions at 3300 and 1730 cm^{-1} are corresponding to the stretching vibration of N$-$H and C=O stretching vibration of benzyl ester group, respectively. The characteristic peaks at 1550 and 1320 cm^{-1} are assigned to amide II and III bands, respectively [29].
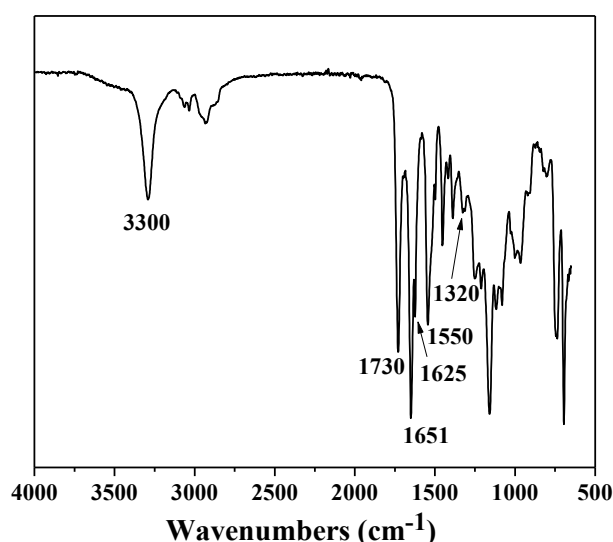

Figure 3. Fourier transform infrared (FTIR) spectrum of PBLG-PPG-PBLG.

The thermal properties of the obtained PBLG-PPG-PBLG film were measured by DSC and TGA. Figure 4 shows the DSC curve of the PBLG-PPG-PBLG film during heating and cooling. Only one glass transition temperature (T_g) was clearly observed, corresponding to the PBLG units [30]. The T_g taken

from the first heating curve was higher than one from the second heating curve (26 °C). Additionally, the sample shows an endothermic peak around $T_m = 100$ °C in the first heating process, which may be due to α-helical transition [30,31]. Figure 5 displays the TGA analysis of the PBLG-PPG-PBLG film. The sample began to decompose at above 280 °C, as evidenced by the rapid decrease in weight, indicating good thermal stability. Mechanical property of the resulting PBLG-PPG-PBLG film was examined by tensile test. Figure 6 exhibits the stress-strain curve, and its tensile strength, elongation and Young's modulus are 8.0 MPa, 13.1%, and 208 MPa, respectively.
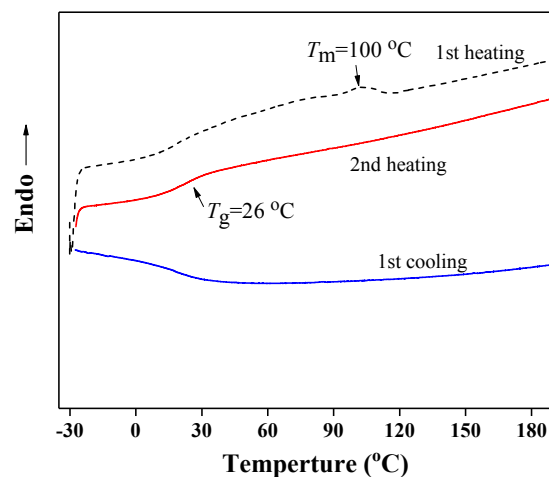

Figure 4. Differential scanning calorimetry (DSC) curves of the obtained PBLG-PPG-PBLG film during heating and cooling.
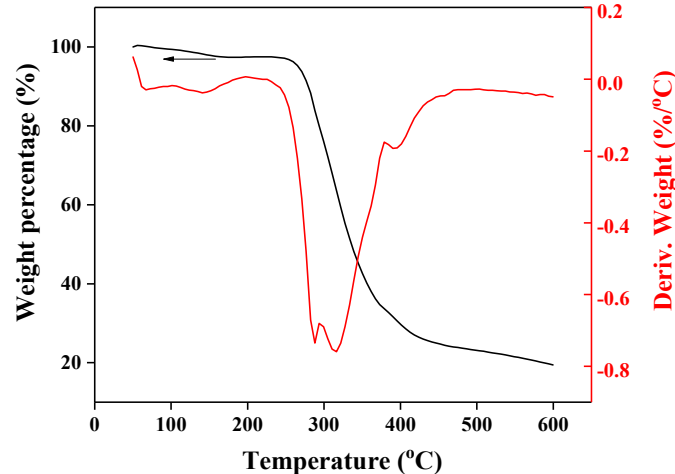

Figure 5. Thermogravimetric analysis (TGA) curve of the PBLG-PPG-PBLG film.

The shape memory properties of the obtained PBLG-PPG-PBLG film were quantitatively evaluated by the bending test. The straight specimen was bent into a "U"-like shape at 100 °C, then cooled down to room temperature with an external force to maintain the deformation. After that, the recovery process was recorded with time at 100 °C, as shown in Figures 7 and 8. The shape fixity ratio (R_f) was close to 100%, and the shape recovery ratio (R_r) inceased with time, which reached ~100% after only 120 s. Furthermore, recovery process of the spiral deformed sample at 100 °C was also investigated, as shown in Figure 9. A full recovery was observed after 240 s. The high R_f and R_r may be due to the existing β-sheet structures as netpoints [16]. The synthesized PBLG-PPG-PBLG exhibits good shape memory behavior, which are promisingly applied in many biomedical applications.
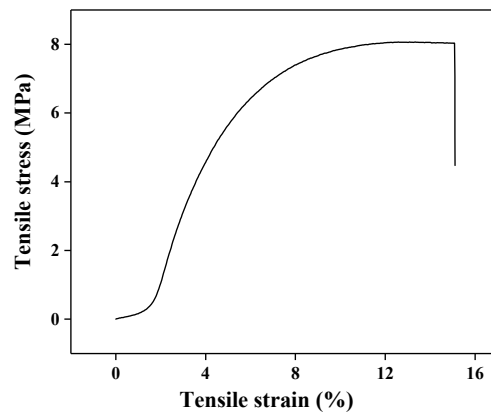
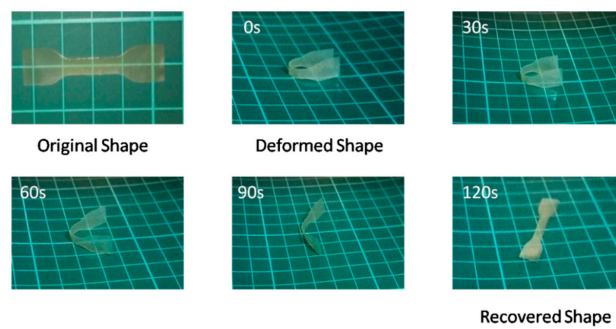**Figure 6.** Stress-strain curve of the obtained PBLG-PPG-PBLG film.

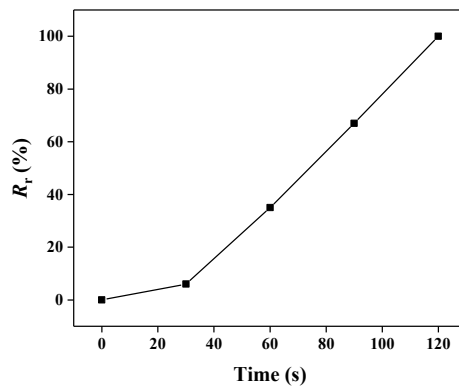**Figure 7.** Shape memory process of the PBLG-PPG-PBLG film at 100 °C.

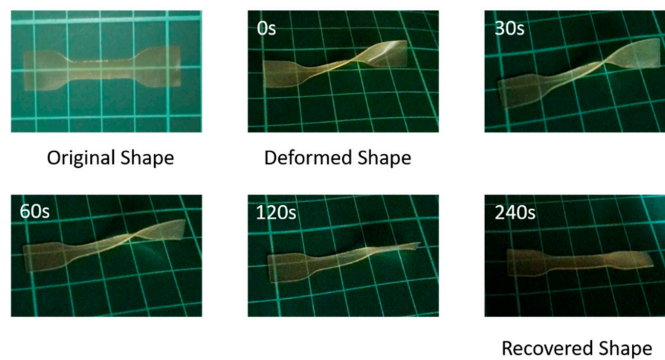**Figure 8.** The plot of shape recovery ratio (R_r) versus recovery time.

Figure 9. Recovery process of the spiral-deformed PBLG-PPG-PBLG film at 100 °C.

4. Conclusions

Shape memory PBLG-PPG-PBLG material was synthesized by ring-opening polymerization of BLG-NCA with PPG-diamine as a macroinitiator. PBLG-PPG-PBLG shows both *α*-helical and *β*-sheet conformations, and the percent of *β*-sheet conformation was about 5.12%, as evidenced by FTIR. It exhibits good shape memory behavior, its shape recovery time is less than 120 s, and its shape fixity ratio and recovery rate could reach ~100%. Further work is being undertaken to achieve better mechanical properties and shape memory mechanisms of PBLG-PPG-PBLG. We believe this work will provide new insight for the development of intelligent polypeptide materials, which will be used in many biomedical applications.

Author Contributions: Lin Gu and Jinlian Hu conceived and designed the experiments; Yuanzhang Jiang and Lin Gu performed the experiments; Lin Gu and Yuanzhang Jiang analyzed the data; Lin Gu wrote the paper.

Conflicts of Interest: The authors declare no conflict of interest.

References

1. Xie, R.; Hu, J.; Ng, F.; Tan, L.; Qin, T.; Zhang, M.; Guo, X. High performance shape memory foams with isocyanate-modified hydroxyapatite nanoparticles for minimally invasive bone regeneration. *Ceram. Int.* **2017**, *43*, 4794–4802. [CrossRef]
2. Gu, L.; Cui, B.; Wu, Q.-Y.; Yu, H. Bio-based polyurethanes with shape memory behavior at body temperature: Effect of different chain extenders. *RSC Adv.* **2016**, *6*, 17888–17895. [CrossRef]
3. Shi, S.; Wu, Q.-Y.; Gu, L.; Zhang, K.; Yu, H. Bio-based (co)polylactide-urethane networks with shape memory behavior at body temperature. *RSC Adv.* **2016**, *6*, 79268–79274. [CrossRef]
4. Chen, C.; Hu, J.; Huang, H.; Zhu, Y.; Qin, T. Design of a Smart Nerve Conduit Based on a Shape-Memory Polymer. *Adv. Mater. Technol.* **2016**, *1*, 1600015. [CrossRef]
5. Wu, Y.; Hu, J.; Zhang, C.; Han, J.; Wang, Y.; Kumar, B. A facile approach to fabricate a UV/heat dual-responsive triple shape memory polymer. *J. Mater. Chem. A* **2015**, *3*, 97–100. [CrossRef]
6. Wu, Y.; Hu, J.; Huang, H.; Li, J.; Zhu, Y.; Tang, B.; Han, J.; Li, L. Memory chromic polyurethane with tetraphenylethylene. *J. Polym. Sci. Part B Polym. Phys.* **2014**, *52*, 104–110. [CrossRef]
7. Wu, Y.; Hu, J.; Han, J.; Zhu, Y.; Huang, H.; Li, J.; Tang, B. Two-way shape memory polymer with "switch–spring" composition by interpenetrating polymer network. *J. Mater. Chem. A* **2014**, *2*, 18816–18822. [CrossRef]
8. Xiao, X.; Qiu, X.; Kong, D.; Zhang, W.; Liu, Y.; Leng, J. Optically transparent high temperature shape memory polymers. *Soft Matter* **2016**, *12*, 2894–2900. [CrossRef] [PubMed]
9. Liu, C.; Qin, H.; Mather, P.T. Review of progress in shape-memory polymers. *J. Mater. Chem.* **2007**, *17*, 1543–1558. [CrossRef]
10. Hager, M.D.; Bode, S.; Weber, C.; Schubert, U.S. Shape memory polymers: Past, present and future developments. *Prog. Polym. Sci.* **2015**, *49–50*, 3–33. [CrossRef]
11. Karger-Kocsis, J.; Kéki, S. Biodegradable polyester-based shape memory polymers: Concepts of (supra)molecular architecturing. *Express Polym. Lett.* **2014**, *8*, 397–412. [CrossRef]
12. Zhu, Y.; Hu, J.; Yeung, K. Effect of soft segment crystallization and hard segment physical crosslink on shape memory function in antibacterial segmented polyurethane ionomers. *Acta Biomater.* **2009**, *5*, 3346–3357. [CrossRef] [PubMed]
13. Zhu, Y.; Hu, J.L.; Yeung, K.W.; Liu, Y.Q.; Liem, H.M. Influence of ionic groups on the crystallization and melting behavior of segmented polyurethane ionomers. *J. Appl. Polym. Sci.* **2006**, *100*, 4603–4613. [CrossRef]
14. Cui, B.; Wu, Q.Y.; Gu, L.; Shen, L.; Yu, H.B. High performance bio-based polyurethane elastomers: Effect of different soft and hard segments. *Chin. J. Polym. Sci.* **2016**, *34*, 901–909. [CrossRef]
15. Hu, J.; Chen, S. A review of actively moving polymers in textile applications. *J. Mater. Chem.* **2010**, *20*, 3346–3355. [CrossRef]

16. Huang, H.; Hu, J.; Zhu, Y. Shape-Memory Biopolymers Based on *β*-Sheet Structures of Polyalanine Segments Inspired by Spider Silks. *Macromol. Biosci.* **2013**, *13*, 161–166. [CrossRef] [PubMed]

17. Deming, T.J. Synthetic polypeptides for biomedical applications. *Prog. Polym. Sci.* **2007**, *32*, 858–875. [CrossRef]

18. Song, Z.; Han, Z.; Lv, S.; Chen, C.; Chen, L.; Yin, L.; Cheng, J. Synthetic polypeptides: From polymer design to supramolecular assembly and biomedical application. *Chem. Soc. Rev.* **2017**, *46*, 6570–6599. [CrossRef] [PubMed]

19. Choi, Y.Y.; Joo, M.K.; Sohn, Y.S.; Jeong, B. Significance of secondary structure in nanostructure formation and thermosensitivity of polypeptide block copolymers. *Soft Matter* **2008**, *4*, 2383–2387. [CrossRef]

20. Lavilla, C.; Byrne, M.; Heise, A. Block-Sequence-Specific Polypeptides from *α*-Amino Acid *N*-Carboxyanhydrides: Synthesis and Influence on Polypeptide Properties. *Macromolecules* **2016**, *49*, 2942–2947. [CrossRef]

21. He, X.; Fan, J.; Wooley, K.L. Stimuli-Triggered Sol-Gel Transitions of Polypeptides Derived from -alpha-Amino Acid *N*-Carboxyanhydride (NCA) Polymerizations. *Chem. Asian J.* **2016**, *11*, 437–447. [CrossRef] [PubMed]

22. Fu, X.; Ma, Y.; Shen, Y.; Fu, W.; Li, Z. Oxidation-Responsive OEGylated Poly-L-cysteine and Solution Properties Studies. *Biomacromolecules* **2014**, *15*, 1055–1061. [CrossRef] [PubMed]

23. Huang, J.; Heise, A. Stimuli responsive synthetic polypeptides derived from *N*-carboxyanhydride (NCA) polymerisation. *Chem. Soc. Rev.* **2013**, *42*, 7373–7390. [CrossRef] [PubMed]

24. Fu, X.; Shen, Y.; Fu, W.; Li, Z. Thermoresponsive Oligo(ethylene glycol) Functionalized Poly-L-cysteine. *Macromolecules* **2013**, *46*, 3753–3760. [CrossRef]

25. Peterson, G.I.; Dobrynin, A.V.; Becker, M.L. Alpha-Amino Acid-Based Poly(Ester urea)s as Multishape Memory Polymers for Biomedical Applications. *ACS Macro Lett.* **2016**, *5*, 1176–1179. [CrossRef]

26. Guo, A.-R.; Yang, W.-X.; Yang, F.; Yu, R.; Wu, Y.-X. Well-Defined Poly(*γ*-benzyl-L-glutamate)-*g*-Polytetrahydrofuran: Synthesis, Characterization, and Properties. *Macromolecules* **2014**, *47*, 5450–5461. [CrossRef]

27. Lee, N.H.; Frank, C.W. Surface-Initiated Vapor Polymerization of Various *α*-Amino Acids. *Langmuir* **2003**, *19*, 1295–1303. [CrossRef]

28. Kotharangannagari, V.K.; Sánchez-Ferrer, A.; Ruokolainen, J.; Mezzenga, R. Thermoreversible Gel–Sol Behavior of Rod–Coil–Rod Peptide-Based Triblock Copolymers. *Macromolecules* **2012**, *45*, 1982–1990. [CrossRef]

29. Yang, W.-X.; Wang, L.-L.; Zhu, H.; Xu, R.-W.; Wu, Y.-X. Synthesis of poly(glutamic acid-co-aspartic acid) VIA combination of *N*-carboxyanhydride ring opening polymerization with debenzylation. *Chin. J. Polym. Sci.* **2013**, *31*, 1706–1716. [CrossRef]

30. Sánchez-Ferrer, A.; Mezzenga, R. Secondary Structure-Induced Micro- and Macrophase Separation in Rod-Coil Polypeptide Diblock, Triblock, and Star-Block Copolymers. *Macromolecules* **2010**, *43*, 1093–1100. [CrossRef]

31. Wei, M.-J.; Guo, A.-R.; Wu, Y.-X. Microstructure and Micromorphology of Poly (*γ*-benzyl-L-glutamate)-*g*-(Polytetrahydrofuran-*b*-Polyisobutylene) Copolymer. *Acta Polym. Sin.* **2017**, *3*, 506–515.